

Methods for the detection of gravitational waves from subsolar mass ultracompact binaries

Ryan Magee,^{1,2} Anne-Sylvie Deutsch,^{1,2} Phoebe McClincy,² Chad Hanna,^{1,2,3} Christian Horst,⁴ Duncan Meacher,^{1,2,4} Cody Messick,^{1,2} Sarah Shandera,^{1,2} and Madeline Wade⁵

¹*Institute for Gravitation and the Cosmos, The Pennsylvania State University, University Park, Pennsylvania 16802, USA*

²*Department of Physics, The Pennsylvania State University, University Park, Pennsylvania 16802, USA*

³*Department of Astronomy and Astrophysics, The Pennsylvania State University, University Park, Pennsylvania 16802, USA*

⁴*University of Wisconsin-Milwaukee, Milwaukee, Wisconsin 53201, USA*

⁵*Kenyon College, Gambier, Ohio 43022, USA*



(Received 16 August 2018; published 30 November 2018)

We describe detection methods for extensions of gravitational wave searches to subsolar mass ultracompact binaries. Subsolar mass searches were previously carried out during the Initial LIGO era, and Advanced LIGO boasts a detection volume approximately 1000 times larger than Initial LIGO at design sensitivity. Low mass compact binary searches present computational challenges, and we suggest a way to mitigate the increased computational cost while retaining a sensitivity much greater than previous searches. Subsolar mass compact objects are of particular interest because they are not expected to form astrophysically. If detected, they could be evidence of primordial black holes or some other yet unknown formation mechanism. We consider a particular model of primordial black hole binary formation that would allow LIGO/Virgo to place constraints on this population within the context of dark matter, and we demonstrate how to obtain conservative bounds for the upper limit on the dark matter fraction.

DOI: [10.1103/PhysRevD.98.103024](https://doi.org/10.1103/PhysRevD.98.103024)

I. INTRODUCTION

Advanced LIGO's [1] and Advanced Virgo's [2] detections of gravitational waves from compact binary coalescences (CBCs) have ushered in the dawn of gravitational wave astronomy. To date, there have been five detections of binary black hole mergers [3–6] and one detection of a binary neutron star system [7], each of which has expanded our knowledge of the properties and populations of compact objects in our Universe. Advanced LIGO's and Advanced Virgo's success in detecting traditional sources of gravitational waves suggests that ground-based interferometers could be powerful new tools in observing the dark Universe. We describe considerations for extensions of traditional compact binary searches to the subsolar mass regime and provide motivation for these searches in the context of dark matter. In particular, we consider a model where a uniform, monochromatic (equal mass) distribution of primordial black holes (PBHs) makes up a fraction of the dark matter. We examine the model's robustness and demonstrate how it can place constraints on the abundance of PBHs for different subsolar mass populations.

II. ANALYSIS TECHNIQUES

Advanced LIGO compact binary searches rely on matched filtering to extract candidate signals from the

noise by correlating known gravitational waveforms with the data. Compact binary searches currently require $\mathcal{O}(10^5)$ – $\mathcal{O}(10^6)$ templates to adequately recover arbitrary signals placed in the parameter spaces considered thus far (binary systems with a total mass of $2 M_{\odot}$ – $600 M_{\odot}$ [8,9]). The addition of fully precessing waveforms in future observing runs could increase this by yet another factor of 10, though for now this remains computationally infeasible.

The difficulty of CBC searches scales with both the number and length of the waveforms used as matched filter templates, which could present a problem for subsolar mass searches. Here, we focus on the effect of the number of templates in the template bank, which is expected to scale (roughly) as

$$N \propto m_{\min}^{-8/3} f_{\min}^{-8/3}, \quad (1)$$

where m_{\min} is the minimum mass included in the search and f_{\min} denotes the starting frequency of the template waveforms [10]. Previous Advanced LIGO searches have searched for binaries with components as light as $1 M_{\odot}$ [8,11]; extending these searches to lower masses could easily lead to a 10–100 times increase in difficulty compared to offline analyses in Advanced LIGO's first observing run. Below, we propose increasing f_{\min} to mitigate the increased computational costs associated with

low mass extensions of compact binary searches, and we calculate the expected loss in sensitivity that this brings.

A. Estimates of sensitivity

Second-generation ground-based gravitational wave detectors such as Advanced LIGO and Advanced Virgo are sensitive over a broad range of frequencies (~ 10 – $10\,000$ Hz), but they are most sensitive near 100 Hz [12]. Compact binary pipelines exploit this sensitivity and typically analyze a subset of the total bandwidth. In Advanced LIGO’s first observing run, frequencies spanning 10–2048 Hz were analyzed [13]. This is an excellent approximation for standard CBC searches; the majority of the signal-to-noise ratio (SNR) is accumulated at lower frequencies, and very little sensitivity is lost by cutting the analysis at 2048 Hz. This is an even better approximation for subsolar mass compact binaries since the frequency evolution of a binary goes as [14]

$$\dot{f} \propto \mathcal{M}^{5/3} f^{11/3}, \quad (2)$$

where

$$\mathcal{M} = \frac{(m_1 m_2)^{3/5}}{(m_1 + m_2)^{1/5}} \quad (3)$$

is the chirp mass of the system. Subsolar mass systems therefore are not only long lived but also spend a long time in LIGO’s most sensitive band compared to heavier binaries. This suggests that it may be possible to analyze an even more reduced frequency band than previous searches while retaining a significant amount of SNR.

Since orbital decay is slow for subsolar mass ultra-compact binaries, inspiral only waveforms appropriately approximate the signal received on Earth. The amplitude of the waveform can be written as [15]

$$|\tilde{h}(f)| = \frac{1}{D} \left(\frac{5\pi}{24c^3} \right)^{1/2} (G\mathcal{M})^{5/6} (\pi f)^{-7/6}, \quad (4)$$

and the average recovered signal-to-noise ratio is given by

$$\langle \rho \rangle = \sqrt{4 \int_{f_{\min}}^{f_{\max}} \frac{|\tilde{h}(f)|^2}{S_n(f)} df}, \quad (5)$$

where $S_n(f)$ denotes the single sided power spectral density, informally referred to as the “noise curve.” f_{\min} is determined by either the low frequency noise floor or the starting frequency of the template waveform (whichever is greater), and f_{\max} is determined by the frequency of the innermost stable circular orbit (f_{ISCO}) or the ending frequency of the template waveform (whichever is less), where f_{ISCO} is defined as

$$f_{\text{ISCO}} = \frac{c^3}{6\sqrt{6}\pi G M_{\text{total}}}. \quad (6)$$

For a $1 M_{\odot}$ – $1 M_{\odot}$ binary, $f_{\text{ISCO}} \approx 2200$ Hz. The frequency monotonically increases for lighter total mass systems; for a subsolar mass search, f_{\max} is therefore determined by the bandwidth of the template waveforms.

We can substitute the waveform amplitude into the equation for the SNR and rearrange to find the horizon distance for a given $\langle \rho \rangle$ (or, equivalently, the SNR recovered at some fiducial distance),

$$D_{\max} \propto \frac{1}{\langle \rho \rangle} \mathcal{M}^{5/6} \sqrt{4 \int_{f_{\min}}^{f_{\max}} \frac{f^{-7/3}}{S_n(f)} df}, \quad (7)$$

which is dependent on the noise curves, the chirp mass of the binary, and the frequency band of the analysis. This allows us to compare LIGO’s sensitivity for frequency bands that do not encompass the full sensitive range. We choose the $f \in (10 \text{ Hz}, 2048 \text{ Hz})$ band as a point of comparison. The fraction of the SNR retained is then

$$f_{\text{SNR}} = \frac{D(f_{\min}, f_{\max})}{D(10 \text{ Hz}, 2048 \text{ Hz})}. \quad (8)$$

Note that this fractional reduction is independent of the mass of the binary. This presents an important trade-off in subsolar mass searches: increasing f_{\min} drives the difficulty of a search down, but it also causes the search to lose sensitivity. This drop in the SNR is equivalent to a fractional decrease in LIGO’s average range, which means that the observed volume (and therefore the expected number of detections at a given chirp mass) is smaller by a factor of f_{SNR}^3 . Thus, even a 3% loss in the SNR would represent a detection volume nearly 10% smaller. The sensitive volume retained as a function of f_{\min} and f_{\max} is shown in Fig. 1.

B. Sensitive distance

Initial LIGO previously carried out searches for compact binaries with components as light as $0.2 M_{\odot}$ [22]. Using the relations outlined above and the fact that current Advanced LIGO searches extend to $1 M_{\odot}$ and $f_{\min} = 10$ Hz, we can estimate the reduction in frequency band and sensitivity required to keep the cost of a subsolar mass search comparable to current Advanced LIGO searches. Equation (1) shows that we expect similar scalings in both m_{\min} and f_{\min} . Thus, if we decrease the lower mass bound of previous Advanced LIGO searches by a factor of 5, we need to *increase* f_{\min} by a factor of 5 as well to keep the number of templates approximately constant. We estimate that in order to modify current searches to extend down to this mass we would need to increase f_{\min} to ~ 50 Hz. This amounts to a loss of 10% in the SNR and range, and therefore a loss of $\sim 30\%$ in the volume and detection rate. The Initial LIGO subsolar mass searches also made use of a reduced frequency band. The lowest mass binary considered in those

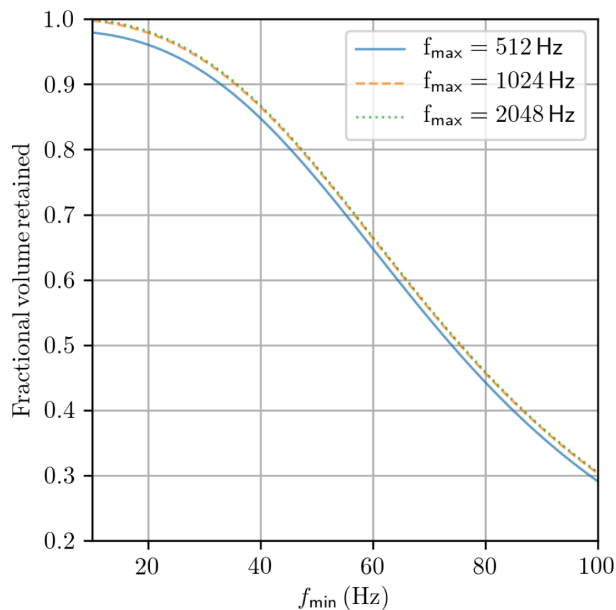


FIG. 1. The fractional volume retained for various values of f_{\max} and as a function of f_{\min} . The dotted, dashed, and solid lines correspond to upper cutoff frequencies of 2048, 1024, and 512 Hz, respectively. Note that there is very little difference between the various f_{\max} values; this is because there is more than an order of magnitude more noise at these frequencies than the in ~ 100 Hz region and a very little SNR is accumulated there. All values are measured relative to the band $f \in (10 \text{ Hz}, 2048 \text{ Hz})$.

searches remained visible at a range of ~ 4 Mpc [23]. We estimate that for the same mass and for the frequency band suggested above Advanced LIGO has a range of ~ 58 Mpc, which corresponds to a sensitive volume 3 orders of magnitude greater. An estimate of Advanced LIGO's range using the full frequency band is shown in Fig. 2.

C. Approximation of the merger rate for null results

We can estimate the upper limit on the merger rate in the event of a null result using a combination of the methods outlined above. In Eq. (7), we defined the horizon distance of the detector. This represents the maximum distance for which an optimally located and oriented source would be recovered with some $\langle \rho \rangle$. In general, however, detectors will measure a weaker response to a gravitational wave depending on the location and orientation of the binary. This reduction is described by the antenna patterns, F_+ and F_\times , which always take values less than or equal to 1 and are related to the signal observed on Earth through

$$h = F_+ h_+ + F_\times h_\times. \quad (9)$$

Averaging the detector response over both the location and orientation of the binary reduces the strain recovered (and therefore the distance to a binary with some fiducial $\langle \rho \rangle$) by a factor of 2.26 [24–26]. This can be used to define the average range of the detector as

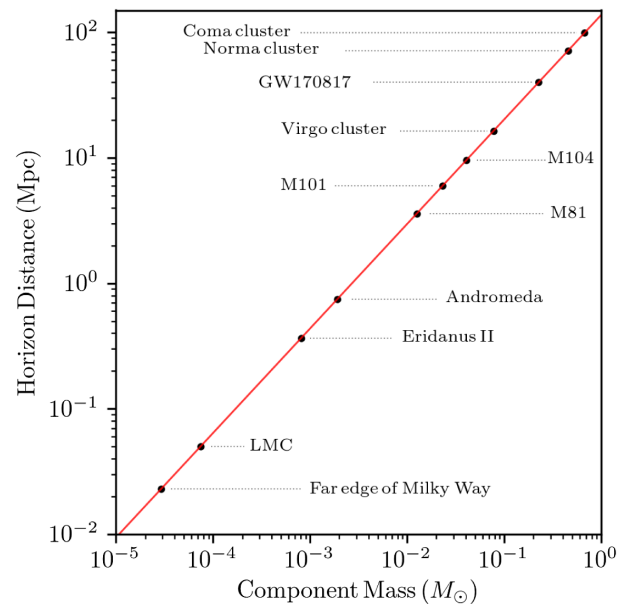


FIG. 2. The distance to an optimally oriented, equal mass binary shown as a function of the component mass. LIGO remains sensitive to $\mathcal{O}(10^{-5} M_\odot - 10^{-5} M_\odot)$ binaries at extra-galactic distances. This plot assumes $f_{\min} = 10 \text{ Hz}$ and $f_{\max} = 2048 \text{ Hz}$ and therefore represents an optimistic view of horizon distance and ignores search difficulty. Nevertheless, this demonstrates that LIGO is capable of detecting extremely low mass ultracompact binaries at extra-galactic distances; understanding the scaling of subsolar mass searches is crucial if we wish to probe that mass range. Astrophysical galaxies, groups, and clusters are included as a reference for cosmological distances. Several objects previously considered as observational candidates for the abundance of dark matter (Eridanus II, LMC/SMC, and Segue I) are well within LIGO's range at low masses. Approximate distances are taken from Refs. [7, 16–21]. The noise curve used to approximate sensitivity in Advanced LIGO's first observing run (O1) sensitivity is “Early high/Mid low” from Ref. [12].

$$D_{\text{avg}} = \frac{D_{\text{max}}}{2.26}. \quad (10)$$

The average sensitive distance allows us to approximate limits on the coalescence rate from null results for a general gravitational wave search. The loudest event statistic formalism [27] states that we can constrain the binary merger rate for a specific mass bin, i , to 90% confidence with

$$\mathcal{R}_{90,i} = \frac{2.3}{\langle VT \rangle_i}. \quad (11)$$

We can estimate the sensitive volume time for a particular observing run using the earlier range approximation.

$$\langle VT \rangle_i = \frac{4}{3} \pi D_{\text{avg},i}^3 T, \quad (12)$$

where T is the analyzable live time of the two detectors. This method provides an excellent approximation of the sensitive

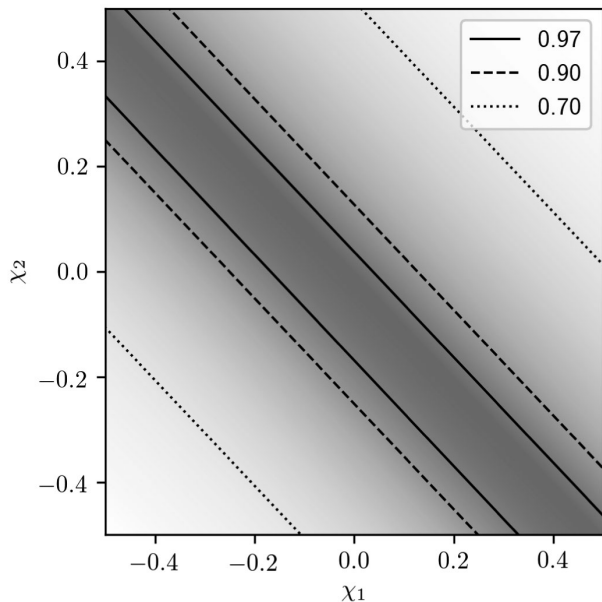


FIG. 3. Recovery of spinning signals with a family of non-spinning template waveforms. Shown in black are lines of constant fitting factor (i.e., the maximum overlap between template waveforms and the injected signals) with the value specified by the line type. The shading shows how the fitting factor changes with the spin of the components in regions between the contours. While systems with $-0.084 < \chi_{\text{eff}} < 0.019$ are recovered well, the match between the two waveforms drops rapidly for χ_{eff} outside this range. The SNR is proportional to the fitting factor, so the loss in the SNR grows rapidly with total spin.

4-volume. The remaining plots in this paper use this procedure to estimate LIGO rates and LIGO sensitivity in the subsolar mass region.

D. Nonspinning waveforms

While reducing the frequency band is one way to mitigate the increased computational cost of subsolar mass searches, nonspinning waveforms also offer an easy way to reduce the difficulty by potentially 1–2 orders of magnitude. There are some theoretical justifications for non-spinning searches: some models predict subsolar mass black holes to be predominately slowly spinning [28], and LIGO’s previous detections have been consistent with low χ_{eff} binaries. Regardless, a completely nonspinning binary is clearly a nonphysical assumption. The efficacy of using nonspinning waveforms to recover spinning waveforms has been examined before [29–31]. In particular, Ref. [29] examined neutron star systems and found that nonspinning templates recovered aligned spin binary neutron stars to the desired level only for $-0.2 \lesssim \chi_{\text{eff}} \lesssim 0$.

We performed a similar test on a population of $0.5 M_{\odot}$ – $0.5 M_{\odot}$ binary black holes, shown in Fig. 3. We created a nonspinning template bank covering component masses $m_i \in (0.3 M_{\odot}, 0.7 M_{\odot})$ using TAYLORF2

waveforms [30,32]. We then injected 10 000 spinning signals into fake data; each signal had spins that were purely aligned or antialigned with the orbital angular momentum and had dimensionless spin values of $|\chi_i| < 0.5$. We then calculated the overlap between our nonspinning template waveforms and the spinning signals. We find results similar to those of Ref. [29]; at low spin, there is a large overlap between the template waveforms and the injected, spinning signals. At higher spins, however, the maximum overlap rapidly falls off, implying that LIGO would miss a significant fraction of the signals with appreciable spin. In fact, we find that the nonspinning bank used here recovers signals well provided $\chi_{\text{eff}} > -0.08$ or $\chi_{\text{eff}} < 0.02$. As χ_{eff} deviates from these values, the fraction of signals missed grows rapidly. A spinning template bank is therefore necessary if subsolar mass ultracompact binaries are either born with appreciable spin components or accrete enough matter to develop substantial spin. We are currently examining the effects of spin on the computational cost of subsolar mass CBC searches, as well as other possible ways to mitigate the increased difficulty of a spinning search.

III. POTENTIAL CONSTRAINTS ON PRIMORDIAL BLACK HOLE ABUNDANCE

While there is a large population of compact objects below one solar mass, the only objects compact enough for detection by LIGO are black holes and neutron stars. Other compact objects begin to coalesce at too low of an orbital frequency to produce gravitational waves in the sensitive band of ground-based interferometers. Neither black holes nor neutron stars are expected to form below one solar mass via known astrophysical mechanisms, though there are models that propose alternative ways to form black holes at this mass [33,34]. It is interesting to consider the possibility that subsolar mass black holes are formed via primordial processes and could be a component of the dark matter. In the event of either a detection or null result, LIGO can provide estimates on the merger rate, so it is therefore necessary to model the binary formation rate for primordial black holes in order to connect LIGO with primordial populations. Here, we describe the sensitivity of one particular model to changes in input parameters as well as the response of constraints on the dark matter fraction, $f_{\text{PBH}} \equiv \Omega_{\text{PBH}}/\Omega_{\text{DM}}$, to changes in merger rate constraints that could be provided by LIGO. We motivate this model as a way to provide a conservative limit on f_{PBH} .

We consider a model of (initially) uniformly distributed, monochromatic black holes formed in the early Universe. A pair of nearest neighbor black holes will start to decouple from the background cosmological expansion and form a binary when the mean energy density in a volume encompassing the two exceeds the background energy density. A third black hole closest to the binary injects angular momentum in the system by applying tidal forces, which ensures that the two black holes will orbit rather than

collide head-on. The resulting expression for the merger rate of primordial black hole binaries in the local Universe is given by

$$\text{event rate} = n_{\text{PBH}} \frac{dP}{dt} \Big|_{t=t_0}. \quad (13)$$

where dP is given by

$$dP = \begin{cases} \frac{3f_{\text{PBH}}^{37}}{58} \left[f_{\text{PBH}}^{-\frac{29}{8}} \left(\frac{t}{t_c} \right)^{\frac{3}{8}} - \left(\frac{t}{t_c} \right)^{\frac{3}{8}} \right] \frac{dt}{t}, & t < t_c \\ \frac{3f_{\text{PBH}}^{37}}{58} \left[f_{\text{PBH}}^{-\frac{29}{8}} \left(\frac{t}{t_c} \right)^{-\frac{1}{7}} - \left(\frac{t}{t_c} \right)^{\frac{3}{8}} \right] \frac{dt}{t}, & t \geq t_c \end{cases} \quad (14)$$

and n_{PBH} is given by

$$n_{\text{PBH}} = \frac{3H_0^2 \Omega_{\text{PBH}}}{8\pi G M_{\text{PBH}}}, \quad (15)$$

where

$$t_c = Q\alpha^4\beta^7\bar{x}^4 f^{25/3} \quad (16)$$

and

$$\bar{x} = \frac{1}{(1+z_{\text{eq}})} (n_{\text{PBH}})^{-1/3} \quad (17)$$

with $Q = 3/170 (GM_{\text{PBH}})^{-3}$, G the gravitational constant, z_{eq} the redshift at matter-radiation equality, and M_{PBH} the mass of each individual black hole in this population. α and β are constants of $\mathcal{O}(1)$ that depend on the dynamics of binary formation and are typically set to 1. This model has been extensively studied [35–39].

This model provides a direct connection between LIGO and PBHs via an expected merger rate which is solely a function of the age of the Universe, t_0 , given some M_{BH} and f_{PBH} . The merger rate is not analytically invertible, but if gravitational wave observations provide a constraint on the merger rate for black holes of a particular mass, then it can be numerically solved to obtain an upper limit on f_{PBH} for that mass bin. Similar procedures have been considered before [37,39].

It is important to consider the robustness of this model and the relative strictness of the constraints it provides. First, consider the effects of varying α and β . Numerical simulations suggest that realistic values are $\alpha = 0.4$, $\beta = 0.8$ [35]. Though not immediately evident from the above equation, smaller values of α and β lead to larger *expected* rates and therefore more stringent estimates of the upper limit of f_{PBH} . The dependence of the expected rate on α and β is shown explicitly in Fig. 4. As α and β dip below 1, the

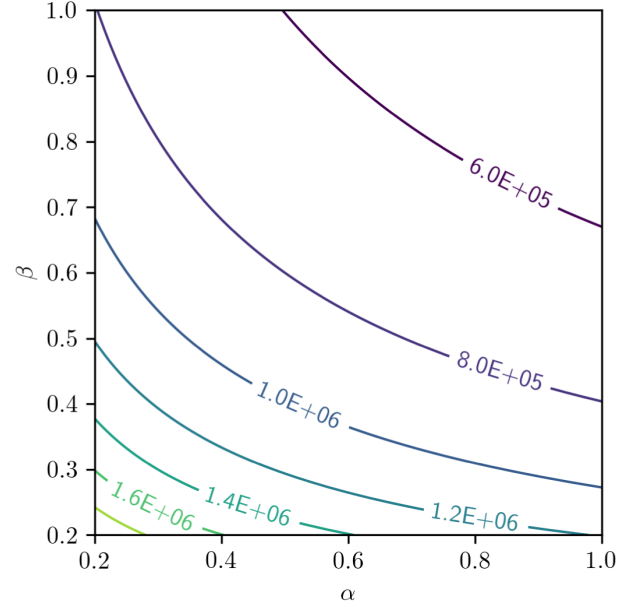


FIG. 4. Merger rate dependence on α and β for a fixed dark matter fraction ($f = 0.5$) and primordial black hole mass ($M_{\text{BH}} = 1.0 M_{\odot}$), shown in units of $\text{Gpc}^{-3} \text{yr}^{-1}$. The expected merger rate strictly increases as either α or β is changed from 1.0. Similar behavior is observed independent of the black hole mass or dark matter fraction. This implies that the constraints on the dark matter fraction that are typically published assuming $\alpha = \beta = 1$ are conservative for this model.

expected merger rate increases. It is a simple extension to approximate how the constraints on f_{PBH} are affected by variations of α and β . We can use the procedure outlined in Sec. II C to approximate the upper limit on the merger rate, which we then invert to find limits on f_{PBH} . We present bounds under this approximation for $\alpha = \beta = 1$ and $\alpha = 0.4$, $\beta = 0.8$ in Fig. 5(a). This figure shows a general feature of the model: as either α or β is decreased, the constraint on f_{PBH} for a given upper bound on the merger rate becomes tighter. Thus, $\alpha = \beta = 1$ provides a more conservative limit on f_{PBH} .

Of course, allowing α and β to increase beyond 1 yields looser constraints. At the time when two PBHs become gravitationally bound to one another, α describes the ratio between the semimajor axis of the binary and the initial physical separation of the two PBHs at the moment they become bound. It is therefore unphysical to expect $\alpha > 1$. β helps to determine the minimum ellipticity of the binary; for $\beta > 1$, the ellipticity becomes imaginary. $\alpha = \beta = 1$ therefore provides the *most* conservative rate estimate for this model.

Another important consideration is the sensitivity of this model to errors in observational measurements of the merger rate. We can propagate errors in rates measurements through to the dark matter fraction. From our upper limit on the merger rate estimate, we find that $f_{\text{PBH}} \approx .28$ at $0.2 M_{\odot}$ and $f_{\text{PBH}} \approx .04$ at $1.0 M_{\odot}$. If we allow for a 50% error in

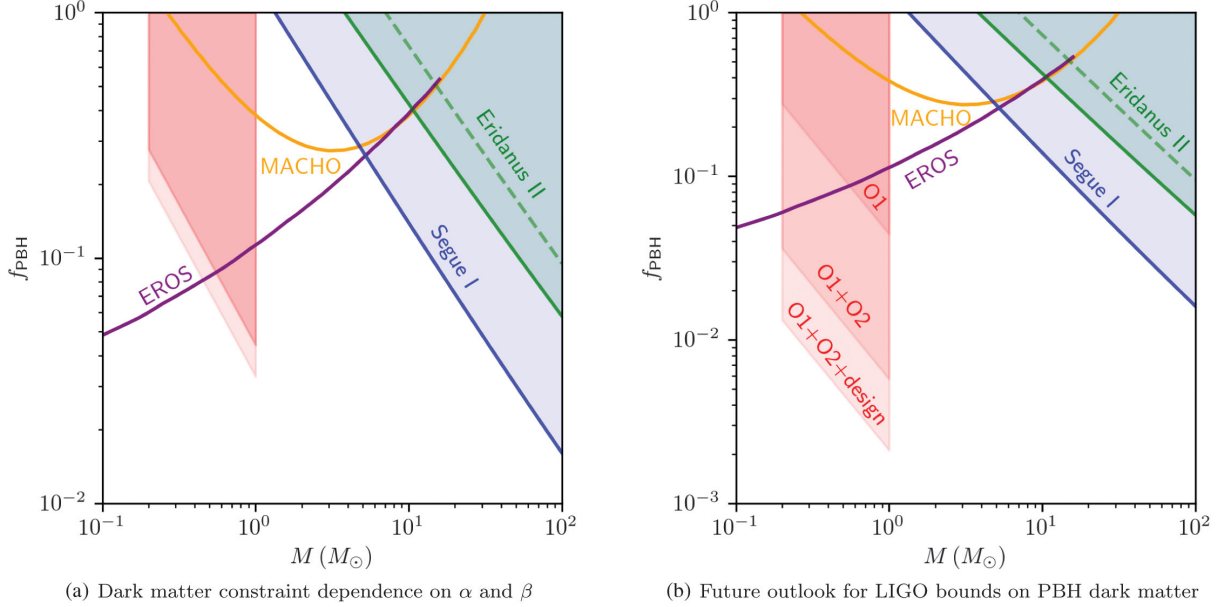


FIG. 5. (a) Limits on the fraction of dark matter composed of primordial black holes in a monochromatic distribution. Shown in purple, yellow, blue, and green are reproductions of the constraints found in Refs. [40–43], respectively. Unlike in Ref. [44], the LIGO limits presented here are based on horizon distance estimates using the power spectra and the loudest event statistic [15,27]. This method is described in the text. Potential LIGO results shown in red emphasize the small effect α and β have on the constraints. The bottom line shows the limit for $\alpha = 0.4, \beta = 0.8$, while the upper line shows $\alpha = \beta = 1$. (b) A possible outlook to the future. Shown here are constraints derived from the same formalism (and assuming continued null results). We follow the procedure mentioned in the text to approximate the rates constraints. Here, we assume year-long runs operating at 40% efficiency for Advanced LIGO’s second observing run (O2) and design contributions. LIGO will be able to place percent level limits on the fraction of dark matter in PBHs after a year of operating at design sensitivity. The noise curves used for this plot come from the data release associated with Ref. [12], specifically the “Early high/Mid low” column for O1, “Mid high/Late low” for O2, and “Design” for design.

the merger rate estimate that this procedure provides, we still find $f \in (.17, .37)$ and $f \in (.03, .06)$ for the respective mass bins, thus demonstrating that the constraints are relatively insensitive to even large errors in the upper bound on the merger rate.

There are several other assumptions made in this model that we do *not* attempt to quantify but instead provide a brief qualitative argument on their effects. First, we have assumed that primordial black holes are uniformly distributed in space. In reality, we expect PBHs to cluster to some extent, which would change the expected event rate for PBH binary mergers. Clustering would tend to increase the amount of binary coalescences, however, so the expected event rate would rise, and therefore the maximum permissible fraction, f_{PBH} , would decrease. Therefore, a spatially uniform distribution of PBHs provides a conservative bound on f_{PBH} . We also ignore the binary’s evolution between formation and coalescence as well as the possibility of late-Universe binary formation. For a discussion of these effects, which appear to be subdominant (though they also drive the expected rate up), see Ref. [45]. A potentially larger effect comes from the assumption of a purely monochromatic distribution of black holes. Though the framework for this formation model has been extended to the unequal mass case in

Ref. [35], we have not considered those effects here. Finally, we also ignore the effects of spin on binary formation.

IV. FUTURE PROSPECTS AND DISCUSSION

As Advanced LIGO approaches design sensitivity, its horizon distance should increase by a factor of 2–3 [46]. This, coupled with more observation, means that LIGO could conceivably have a (cumulative) sensitive $\langle VT \rangle$ $\mathcal{O}(10)$ times larger than was observed in Ref. [44]. Figure 5(b) shows projections for how continued null results could contribute to constraints on f_{PBH} for this mass range. Ground-based interferometers have the unique ability to strengthen bounds in the subsolar mass regime by systematics independent of previous microlensing observations [40,41,47]. This is especially important in light of recent criticisms [48] and studies of the model dependencies of these surveys [49].

There are many areas in which subsolar mass searches can improve on the suggestions outlined here. The most obvious are extensions to lower masses and spinning binaries, each of which presents its own challenges. Lower masses require denser template banks, and they persist in LIGO’s sensitive band longer. One possible solution could be to alter the width of the frequency band

considered for different mass bins, thus stitching together a suitable template bank. Spin is more difficult to incorporate; early tests seem to imply at least a factor of 10 more templates would be required for fully spinning binaries. Examining smaller component spins, such as $\chi_i < 0.3$, could remain computationally feasible and help to mitigate the rapid fall-off in sensitivity that nonspinning banks currently experience for moderate to high spin systems. We are actively pursuing extensions in these areas.

More careful PBH population modeling is also a necessity. In particular, a careful consideration of extended PBH distributions will offer more accurate and general merger rate predictions. Not only will this allow for more precise constraints, but it will also be useful in examining the feasibility of detecting preferred PBH distributions peaked in this mass range. While this paper has demonstrated that the

model considered typically provides a conservative estimate of the bounds on f_{PBH} , a more general formalism will allow testing of different inflationary models.

ACKNOWLEDGMENTS

Funding for this project was provided by the Charles E. Kaufman Foundation of The Pittsburgh Foundation. Computing resources and personnel for this project were provided by Pennsylvania State University. We thank the LIGO Compact Binary Coalescence working group and John Whelan, Nelson Christensen, and Graham Woan for many useful questions and comments. We thank Kipp Cannon for suggesting we consider nonspinning searches in the mass range considered.

-
- [1] J. Aasi *et al.* (LIGO Scientific Collaboration), Advanced LIGO, *Classical Quantum Gravity* **32**, 115012 (2015).
 - [2] F. Acernese *et al.*, Advanced Virgo: A second-generation interferometric gravitational wave detector, *Classical Quantum Gravity* **32**, 024001 (2015).
 - [3] B. P. Abbott *et al.*, GW151226: Observation of Gravitational Waves from a 22-Solar-Mass Binary Black Hole Coalescence, *Phys. Rev. Lett.* **116**, 241103 (2016).
 - [4] B. P. Abbott *et al.*, GW170104: Observation of a 50-Solar-Mass Binary Black Hole Coalescence at Redshift 0.2, *Phys. Rev. Lett.* **118**, 221101 (2017).
 - [5] B. P. Abbott *et al.*, GW170608: Observation of a 19-solar-mass binary black hole coalescence, *Astrophys. J.* **851**, L35 (2017).
 - [6] B. P. Abbott *et al.*, GW170814: A Three-Detector Observation of Gravitational Waves from a Binary Black Hole Coalescence, *Phys. Rev. Lett.* **119**, 141101 (2017).
 - [7] B. P. Abbott *et al.*, GW170817: Observation of Gravitational Waves from a Binary Neutron Star Inspiral, *Phys. Rev. Lett.* **119**, 161101 (2017).
 - [8] B. P. Abbott *et al.*, Binary black hole mergers in the first Advanced LIGO Observing Run, *Phys. Rev. X* **6**, 041015 (2016).
 - [9] B. P. Abbott *et al.*, Search for intermediate mass black hole binaries in the first observing run of Advanced LIGO, *Phys. Rev. D* **96**, 022001 (2017).
 - [10] B. J. Owen and B. S. Sathyaprakash, Matched filtering of gravitational waves from inspiraling compact binaries: Computational cost and template placement, *Phys. Rev. D* **60**, 022002 (1999).
 - [11] B. P. Abbott *et al.*, Upper limits on the rates of binary neutron star and neutron star-black hole mergers from advanced Ligo's first observing run, *Astrophys. J.* **832**, L21 (2016).
 - [12] B. P. Abbott *et al.*, Sensitivity of the Advanced LIGO detectors at the beginning of gravitational wave astronomy, *Phys. Rev. D* **93**, 112004 (2016); *Publisher's Note* **97**, 059901 (2018).
 - [13] C. Messick *et al.*, Analysis framework for the prompt discovery of compact binary mergers in gravitational-wave data, *Phys. Rev. D* **95**, 042001 (2017).
 - [14] C. Cutler and E. E. Flanagan, Gravitational waves from merging compact binaries: How accurately can one extract the binary's parameters from the inspiral wave form?, *Phys. Rev. D* **49**, 2658 (1994).
 - [15] J. Abadie *et al.*, Sensitivity to gravitational waves from compact binary coalescences achieved during LIGO's fifth and Virgo's first science run, LIGO Technical Document No. LIGO-T0900499-V19, 2010.
 - [16] S. Mei, J. Blakeslee, P. Cote, J. Tonry, M. J. West, L. Ferrarese, A. Jordan, E. Peng, A. Anthony, and D. Merritt, The ACS Virgo cluster survey. 13. SBF distance catalog and the three-dimensional structure of the Virgo cluster, *Astrophys. J.* **655**, 144 (2007).
 - [17] G. Pietrzyński *et al.*, An eclipsing binary distance to the Large Magellanic Cloud accurate to 2 per cent, *Nature (London)* **495**, 76 (2013).
 - [18] F. Vilardeell, I. Ribas, C. Jordi, E. L. Fitzpatrick, and E. F. Guinan, The distance to the Andromeda galaxy from eclipsing binaries, *Astron. Astrophys.* **509**, A70 (2010).
 - [19] D. Carter *et al.*, The HST/ACS Coma Cluster Survey: I—Survey objectives and design, *Astrophys. J. Suppl. Ser.* **176**, 424 (2008).
 - [20] J. R. Gerke, C. S. Kochanek, J. L. Prieto, K. Z. Stanek, and L. M. Macri, A study of Cepheids in M81 with the large binocular telescope (efficiently calibrated with hubble space telescope), *Astrophys. J.* **743**, 176 (2011).
 - [21] T. Mutabazi, S. L. Blyth, P. A. Woudt, J. R. Lucey, T. H. Jarrett, M. Bilicki, A. C. Schroder, and S. A. W. Moore, The Norma cluster (ACO 3627)—III. The distance and peculiar velocity via the near-infrared Ks-band

- fundamental plane, *Mon. Not. R. Astron. Soc.* **439**, 3666 (2014).
- [22] B. Abbott *et al.*, Search for gravitational waves from primordial black hole binary coalescences in the galactic halo, *Phys. Rev. D* **72**, 082002 (2005).
- [23] B. Abbott *et al.*, Search for gravitational waves from binary inspirals in S3 and S4 LIGO data, *Phys. Rev. D* **77**, 062002 (2008).
- [24] L. S. Finn and D. F. Chernoff, Observing binary inspiral in gravitational radiation: One interferometer, *Phys. Rev. D* **47**, 2198 (1993).
- [25] J. Abadie *et al.*, Predictions for the rates of compact binary coalescences observable by ground-based gravitational-wave detectors, *Classical Quantum Gravity* **27**, 173001 (2010).
- [26] P. Sutton, S3 performance of the LIGO interferometers as measured by sensemonitor, **27**, (2003), LIGO-T030276-x0.
- [27] R. Biswas, P. R. Brady, J. D. E. Creighton, and S. Fairhurst, The loudest event statistic: General formulation, properties and applications, *Classical Quantum Gravity* **26**, 175009 (2009); Corrigendum: The loudest event statistic: General formulation, properties and applications, *Classical Quantum Gravity* **30**, 079502 (2013).
- [28] T. Chiba and S. Yokoyama, Spin distribution of primordial black holes, *Prog. Theor. Exp. Phys.* **2017**, 083E01 (2017).
- [29] H.-S. Cho and C.-Hwan Lee, Gravitational wave searches for aligned-spin binary neutron stars using nonspinning templates, *J. Korean Phys. Soc.* **72**, 1 (2018).
- [30] C. Capano, I. Harry, S. Privitera, and A. Buonanno, Implementing a search for gravitational waves from binary black holes with nonprecessing spin, *Phys. Rev. D* **93**, 124007 (2016).
- [31] T. Dal Canton *et al.*, Implementing a search for aligned-spin neutron star-black hole systems with advanced ground based gravitational wave detectors, *Phys. Rev. D* **90**, 082004 (2014).
- [32] P. Ajith, N. Fotopoulos, S. Privitera, A. Neunzert, and A. J. Weinstein, Effectual template bank for the detection of gravitational waves from inspiralling compact binaries with generic spins, *Phys. Rev. D* **89**, 084041 (2014).
- [33] S. Shandera, D. Jeong, and H. S. Grasshorn Gebhardt, Gravitational Waves from Binary Mergers of Sub-Solar Mass Dark Black Holes, *Phys. Rev. Lett.* **120**, 241102 (2018).
- [34] C. Kouvaris, P. Tinyakov, and M. H. G. Tytgat, Non-primordial solar mass black holes, 2018.
- [35] K. Ioka, T. Chiba, T. Tanaka, and T. Nakamura, Black hole binary formation in the expanding Universe: Three body problem approximation, *Phys. Rev. D* **58**, 063003 (1998).
- [36] T. Nakamura, M. Sasaki, T. Tanaka, and K. S. Thorne, Gravitational waves from coalescing black hole MACHO binaries, *Astrophys. J.* **487**, L139 (1997).
- [37] M. Sasaki, T. Suyama, T. Tanaka, and S. Yokoyama, Primordial Black Hole Scenario for the Gravitational-Wave Event GW150914, *Phys. Rev. Lett.* **117**, 061101 (2016).
- [38] Yu. N. Eroshenko, Gravitational waves from primordial black holes collisions in binary systems, *J. Phys. Conf. Ser.* **1051**, 012010 (2018).
- [39] S. Wang, Y.-F. Wang, Q.-G. Huang, and T. G. F. Li, Constraints on the Primordial Black Hole Abundance from the First Advanced LIGO Observation Run Using the Stochastic Gravitational-Wave Background, *Phys. Rev. Lett.* **120**, 191102 (2018).
- [40] P. Tisserand *et al.*, Limits on the Macho content of the galactic halo from the EROS-2 Survey of the Magellanic clouds, *Astron. Astrophys.* **469**, 387 (2007).
- [41] R. A. Allsman *et al.*, MACHO project limits on black hole dark matter in the 1-30 solar mass range, *Astrophys. J.* **550**, L169 (2001).
- [42] S. M. Koushiappas and A. Loeb, Dynamics of Dwarf Galaxies Disfavor Stellar-Mass Black Holes as Dark Matter, *Phys. Rev. Lett.* **119**, 041102 (2017).
- [43] T. D. Brandt, Constraints on MACHO dark matter from compact stellar systems in ultra-faint dwarf galaxies, *Astrophys. J.* **824**, L31 (2016).
- [44] B. P. Abbott *et al.*, Search for subsolar mass ultracompact binaries in advanced LIGO's first observing run, *arXiv*: 1808.04771.
- [45] Y. Ali-Haïmoud, E. D. Kovetz, and M. Kamionkowski, Merger rate of primordial black-hole binaries, *Phys. Rev. D* **96**, 123523 (2017).
- [46] B. P. Abbott *et al.*, Prospects for observing and localizing gravitational-wave transients with advanced LIGO, advanced Virgo and KAGRA, *Living Rev. Relativity* **21**, 3 (2018); **19**, 1 (2016).
- [47] L. Wyrzykowski *et al.*, The OGLE view of microlensing towards the Magellanic Clouds. III. Ruling out sub-solar MACHOs with the OGLE-III LMC data, *Mon. Not. R. Astron. Soc.* **413**, 493 (2011).
- [48] M. R. S. Hawkins, A new look at microlensing limits on dark matter in the Galactic halo, *Astron. Astrophys.* **575**, A107 (2015).
- [49] A. M Green, Astrophysical uncertainties on stellar microlensing constraints on multi-Solar mass primordial black hole dark matter, *Phys. Rev. D* **96**, 043020 (2017).